**Supporting Information**

# *In Situ* Controlled and Conformal Coating of Polydimethylsiloxane Foams with Silver Nanoparticle Networks with Tunable Piezo-Resistive Properties

*Alessandro Paghi, Martina Corsi, Samuele Corso, Stefano Mariani, and Giuseppe Barillaro**

Dipartimento di Ingegneria dell'Informazione, Università di Pisa, via G. Caruso 16, 56122 Pisa, Italy

*corresponding author: giuseppe.barillaro@unipi.it

## Materials and Methods

### Materials and chemicals

PDMS (polydimethylsiloxane) Sylgard 184 base and thermal curing agent were purchased from Cecchi S.R.L. (Firenze, Italy). Ethanol (99.9 wt%) were purchased from CARLO ERBA Reagents (Milan, Italy). Sodium Chloride (NaCl, 99%), Silver Fluoride (AgF, 99.9%), and Hydrofluoric acid (HF, 48 %) were purchased from Merck Life Science S.R.L (Italy). Aqueous solutions were prepared using deionized water (DIW, 18 MΩ×cm) filtered by Elix® (Merck Millipore, Germany). Adhesive and flexible copper tape (HB 720A Hi-Bond) was purchased from RS Components S.R.L. (Italy). Self-adhesive medical tape (Leukoplast, BSN medical GmbH, Germany) was purchased from Farmacia Comunale La Fontina (Pisa, Italy).

### Preparation of PDMS foams

PDMS foams were prepared using NaCl (grain size 278 ± 63 μm) as a sacrificial template. A NaCl:DIW mixture (5:1 w/w) was inserted and compressed into a 20 mL volume, 20 mm diameter syringe (HSW HENKE SASS WOLF S.R.L) and dried in a ventilated oven (BINDER) at 90 °C for 2 hours. PDMS was prepared by mixing base and curing agents (10:1 w/w). A mass of 15 g of the mix was poured in a polystyrene Petri dish (9 cm in diameter) and then vacuumed for 30 min using

a rotation pump to remove air bubbles trapped in the PDMS mixture [1]. The PDMS was then vacuum-assisted infiltrated into the syringe with NaCl template using a rotary pump to speed up the process, and thermally cured in the oven at 90°C for 5 hours. After curing, NaCl:PDMS cylinders (15.1 mm diameter, 5 mm thickness) were cut using a razor blade and cylindrical puncher. The NaCl template was dissolved by 24−48 hours immersion in DIW:EtOH (10:1 v/v) changing the solution three times per day obtaining the PDMS foams. The PDMS foams were then dried in a ventilated oven at 90 °C for 1 hour. Eventually, the PDMS foams were immersed overnight in EtOH to remove the excess of curing agent and finally dried in a ventilated oven at 90 °C for 30 mins.

**Decoration of PDMS foams with AgNPs**

A solution of 45 mM AgF in EtOH was used for the decoration of PDMS foams. A PDMS foam was inserted into a 10 mL volume, 15 mm diameter syringe (PIKDARE S.P.A.) used to suck 0.9 mL of the AgF:EtOH solution so as to completely fill the PDMS foam (foam volume of about 0.9 ml). The PDMS foam was incubated with the AgF solution (in the syringe) for different times up to a maximum time of 18 hours, at room temperature (i.e., 21°C). The AgF solution in the syringe was changed every hour during the decoration process. After decoration, the AgF solution was ejected from the syringe by squeezing the foam with the piston, then 5 ml of ethanol are pulled in the syringe to rinse the foam. The ethanol is then ejected by squeezing the foam to remove AgF and byproducts (i.e., HF). Three rinsing cycles in ethanol are carried out. The PDMS foam decorated with AgNPs is then extracted from the syringe and dried in a ventilated oven at 90 °C for 30 minutes.

For electrical measurements the AgNP-decorated foams were provided with top and bottom electrodes on opposite sides consisting of flexible and adhesive copper tape.

**AgNP mass measurement**

The AgNP mass loaded in the porous PDMS foam at each decoration time was evaluated as the difference in weight between the AgNP-decorated and bare PDMS foam, using an electronic precision balance (Kern ABS 220-4) with a resolution on 0.1 mg.

**Porosity estimation of PDMS foams**

Porosity of both bare and AgNP-decorated PDMS foams was calculated by gravimetric measurements carried out in air, using eq. 1 for bare and eq. 2 for AgNP-decorated foams:

$$P_{bare\ foam} = \left(1 - \frac{V_{bare\ foam}}{V_{bulk\ foam}}\right) \times 100 \quad (1)$$

$$P_{AgNP\ foam} = \left(1 - \frac{V_{bare\ foam} + V_{Ag}}{V_{bulk\ foam}}\right) \times 100 \quad (2)$$

In eq. 1, $V_{bulk\ foam}$ is the volume of a nonporous (i.e., bulk) PDMS cylinder with same dimension of the PDMS foam ($V_{bulk\ foam} = \pi r^2 h$, where $r$ is the cylinder radius and $h$ is the cylinder heigth), $V_{bare\ foam}$ is the volume of the polymeric part of the porous PDMS foam ($V_{bare\ foam} = \frac{m_{bare\ foam}}{PDMS\ density}$, where $m_{bare\ foam}$ is the measured mass and $PDMS\ density = 965\ mg/cm^3$ is the density of PDMS).

In eq. 2, $V_{Ag}$ is the volume of AgNP loaded ($V_{Ag} = \frac{m_{AgNP}}{Ag\ density}$, where $m_{AgNP}$ is the difference between the mass of the bare foam, namely $m_{bare\ foam}$, and the mass of the foam after decoration with AgNPs, and $Ag\ density = 10490\ mg/cm^3$ is the density of Ag).

**Morphological characterization**

Morphological characterization of PDMS foams decorated with AgNPs was carried out using a scanning electron microscope (FE-SEM, FEI Quanta 450 ESEM FEG) with a 5 kV acceleration voltage at various magnifications, namely, 100×, 50000×, and 100000×.

AgNP equivalent radius, density, and surface coverage were extrapolated from post-processing of the cross-sectional SEM images taken at 100000× using Gwyddion software.

**Dynamic mechanical characterization**

Dynamic mechanical characterization of bare and AgNP-decorated PDMS foams was carried out by cyclic uniaxial compressive tests using a Labview-controlled homemade setup [2]. Briefly, the setup consisted of a 50 N load cell (Omega LCMFD, output 2 mV/min, sensitivity 2.20 mV/V, and accuracy 0.03 N) used to measure the pressure acting on the PDMS foam, a Source Meter Unit (Keithley SMU 2410) used to measure the output voltage of the load cell, a motorized z-axis translation stage used to impose the strain level to the PDMS foam (Sigma Koki, stepping motor SGSP80-20ZF, travel per pulse 0.2 μm, max travel 20 mm, max speed 2 mm/s), and a stepping motor controller used to to finely control the translation stage (Sigma Koki, 2 axis stage controller SHOT-302GS, max number of steps 250, min speed 1 pulse per second, max speed 500 000 pulse per second). A force of 0.4 N was pre-applied to the foam to ensure adhesion of the top and bottom surfaces of the PDMS foams to the translation stage. Stress−strain curves of bare and AgNP-decorated porous PDMS foams were then measured imposing a linear strain (loading/unloading, >5 cycles) at a constant rate of 0.5 or 5 mm $min^{-1}$, with a maximum travel of 3 mm. Elastic modulus and residual energy density of the PDMS foams, both bare and AgNP-decorated, were estimated from the stress−strain curves as a function of the AgNP mass. Specifically, the elastic modulus was evaluated in the linear regions of the stress−strain curve (i.e., in the strain ranges 0 − 10 % and 55 − 60 %) as the slope of the linear function best fitting the experimental data (Figure S3b,c); the residual energy was calculated as the hysteresis area of the stress−strain curves (Figure S3d).

**Static and dynamic electromechanical characterization**

Static piezoresistive properties of the AgNP-decorated PDMS foams were investigated in steady-state conditions through linear-sweep voltammetry at different strain levels, namely, 0, 1, 2.5, 5, 7.5, 10, 20, 40, 50, and 60%.

The strain/stress value was imposed/measured using the homemade setup above-described for the mechanical characterization [2]. An additional SMU (Keithley SMU 2410) was used to bias the AgNP-decorated PDMS foams by application of a voltage through the copper tape contacts placed on the opposite sides of the foams and measuring the current flowing through the foams. To ensure that any mechanical (and, in turn, electrical) transient due to viscoelasticity of the PDMS foams was over, application of a given strain level was followed by a wait time of 60 s before electrical measurements were carried out. A force of 0.4 N was pre-applied to the foam to ensure adhesion of the top and bottom surfaces of the PDMS foams to the translation stage.

Current−voltage curves of the AgNP-decorated PDMS foams for a given strain level were recorded by applying of a voltage sweep (3 cycles) from 0 to 1 V (step of 100 mV, integration time 0.3 s) and recording the current flowing through the foams for each voltage value. The procedure was repeated for 4 consecutive loading/unloading cycles in the strain range 0-60% at the strain levels detailed above. The value of the resistance (R) of the foam versus imposed strain and measured stress level was retrieved by best fitting of the current−voltage curve at the different strain levels with a linear function, considering only the fitting giving an $R^2 > 0.99$. The value of equivalent resistivity ($\rho$) was obtained from the resistance value using the well-known relationship: $\rho = R(S/L)$, where S and L are the cross-section area and length of the foam at any given strain value.

The gauge factor (GF), namely, sensitivity to strain, values were obtained as the slope of the piecewise linear function best fitting normalized resistance variation *vs.* strain experimental data; sensitivity to stress (S) values were calculated as the slope of the piecewise linear function best fitting normalized resistance variation *vs.* stress experimental data. Similarly, taking the current variation as the output parameter, the gauge factor ($GF_I$) values (i.e., sensitivity of the current to strain) were obtained as the slope of the piecewise linear function best fitting normalized current variation *vs.* strain experimental data measured at a bias of 1 V (integration time 0.3 s); sensitivity to stress ($S_I$) values (i.e., sensitivity of the current to stress) were retrieved as the slope of the

piecewise linear function best fitting normalized current variation *vs.* stress experimental data measured at a bias of 1 V (integration time 0.3 s).

For the LoD estimation, the behavior of the foams at small strain levels (up to 2%) was investigated by application of repeated displacement steps of 25, 50, and 100 μm to the AgNP-decorated PDMS foams and the current flowing through the foam was measured in real time at a bias of 1 V (sampling time 30 ms, integration time 100 μs).

Dynamic piezoresistive properties of the AgNP-decorated porous PDMS foams were investigated through cyclic uniaxial compressive tests under constant biasing (1 V), using the same homemade setup above-described for the static piezoresistive characterization. A linear strain (loading/ unloading, minimum 20, maximum 1500 full cycles) at different constant rates, namely, 0.5 and 5 mm/min, and over different strain ranges, namely, 20, 40, and 60%, was applied to the foam. For any tested condition, pressure, current I, and resistance R = 1/I values of the foams were measured over time every 0.1 s (integration time 20 ms).

**Radial Artery Pulse Measurement**

Radial artery pulse measurements were performed by placing the AgNP-decorated PDMS foams on the artery located over the radial styloid of the right wrist of a 26-year-old male. The PDMS decorated with ~19.5 mg of AgNPs was packaged within a commercial plastic bracelet. A 10 mV bias voltage was applied between top and down electrodes of the foam and current variations were measured with a SMU (Keithley 2400) with a sampling time of 30 ms and integration time of 100 μs. Post-processing of the experimental raw data was carried out by application of numeric high pass (cut-off frequency 0.5 Hz) and low pass (cut-off frequency 3.5 Hz) filters.

An informed written consent was obtained from the human volunteer prior to the research.

**Table S1**. Representative examples of state-of-art piezoresistive pressure sensors.

| Material | Preparation Method | Strain/ Pressure Range | Limit of Detection (LOD) | Sensitivity (Range) $S = \frac{\Delta R}{R_0}/\Delta P$, $GF = \frac{\Delta R}{R_0}/\frac{\Delta L}{L_0}$ | Stability Cycles | Response ($t_{RES}$) and Recovery ($t_{REC}$)Times | Application | Ref. |
|---|---|---|---|---|---|---|---|---|
| AgNP-coated PDMS foam | Electroless reduction (in-situ) | 0−60 %<br>0−120 kPa | 4 μm<br>25 Pa | $S_1$=41.4 kPa$^{-1}$ (0−5 kPa)<br>$S_2$=0.28 kPa$^{-1}$ (5−120 kPa)<br>$GF_1$=12.46 (0−7.5 %)<br>$GF_2$=0.55 (7.5 −60 %) | 1500 | $t_{RES}$ = 330 ms<br>$t_{REC}$ =180 ms | Radial artery pulse measurement | This work |
| **Polymeric Foams Coated with Conductive Nanofillers** | | | | | | | | |
| Au film-coated PU foam | Sputtering (in-situ) | 0−60% | 0.568 Pa | $GF_1$=1.09 (0−23%)<br>$GF_2$=1.37 (23−47%)<br>$GF_3$=4.43 (47−60%) | 1000 | $t_{RES}$ = 9 ms<br>$t_{REC}$ N/A | Speech recognition, heart beating | [3] |
| Graphene-coated PU foam | Immersion coating and hydrothemal reduction (ex-situ) | 0−10 kPa | 9 Pa | $S_1$=0.26 kPa$^{-1}$ (0−2 kPa)<br>$S_2$=0.03 kPa$^{-1}$ (2−10 kPa) | 10000 | $t_{RES}$ N/A<br>$t_{REC}$ N/A | Measurement of the spatial pressure distribution | [4] |
| Graphene-coated PU foam | Immersion coating (ex-situ) | 0−640 KPa | 2.3 Pa | $S_1$=1.04 kPa$^{-1}$ (13−260 Pa)<br>$S_2$=0.12 kPa$^{-1}$ (260 Pa−20 kPa) | N/A | $t_{RES}$ = 34 ms<br>$t_{REC}$ = 5 ms | Surface roughness detection | [5] |
| Graphene-coated PU foam | Immersion coating and hydrothemal reduction (ex-situ) | 0−99 % | N/A | S=0.75−3.08 kPa$^{-1}$ (0−15 kPa) | 10000 | $t_{RES}$ = 14 ms<br>$t_{REC}$ N/A | N/A | [6] |
| CNTs-coated PDMS foam | Drop casting (ex-situ) | 0−60 %<br>0−50 kPa | 3 μm<br>6 Pa | $S_1$=0.3 kPa$^{-1}$ (0−1 kPa)<br>$S_2$=0.9 kPa$^{-1}$ (15−50 kPa)<br>$GF_1$=5.6 (0−2.5%)<br>$GF_2$=1.16 (2.5−60%) | 255 | $t_{RES}$ N/A<br>$t_{REC}$ N/A | N/A | [2] |
| CNT/rGO-coated PU foam | Layer-by-layer assembly (ex-situ) | 0−75 %<br>0−5.6 kPa | N/A | GF = 0.96 to 1.75 (0−75%) | N/A | $t_{RES}$ N/A<br>$t_{REC}$ N/A | Finger and elbow bending detection | [7] |
| CNT/rGO-coated PU foam | Immersion coating (ex-situ) | 0−100 %<br>0−48.8 kPa | 3.7 Pa | $S_1$=0.022 kPa$^{-1}$ (0−2.7 kPa) $S_2$=0.088 kPa$^{-1}$ (2.7−10 kPa)<br>$S_3$=0.034 kPa$^{-1}$ (>10 kPa) | 5000 | $t_{RES}$ = 30 ms<br>$t_{REC}$ N/A | Finger bending detection | [8] |
| Carbon black-coated PU foam | Layer-by-layer assembly (ex-situ) | 0 − 60 % | 91 Pa | $S_1$=0.068 kPa$^{-1}$ (0−2 kPa)<br>$S_2$=0.023 kPa$^{-1}$ (2−10 kPa)<br>$S_3$=0.036 kPa$^{-1}$ (10−16 kPa)<br>$GF_1$= 2.2 (0−10%)<br>$GF_2$= -0.38 (10−50%)<br>$GF_3$= -3.1 (50−60%) | 50000 | $t_{RES}$ = 20 ms<br>$t_{REC}$ N/A | Speaking, coughing, swallowing, radial artery pulse breathing detection | [9] |
| rGO/PANi-coated melamine foam | Immersion coating, hydrothemal reduction, PANi polymerization (ex-situ) | 0 − 27 kPa | N/A | $S_1$=0.152 kPa$^{-1}$ (0−3.2 kPa)<br>$S_2$=0.0049 kPa$^{-1}$ (13−27 kPa)<br>$S_3$=0.034 kPa$^{-1}$ (>10 kPa) | 9000 | $t_{RES}$ = 96 ms<br>$t_{REC}$ N/A | Voice recognition, swallowing, blowing, breathing monitoring | [10] |
| PEDOT:PSS-coated melamine foam | Immersion coating (ex-situ) | 0−80 % | N/A | GF=−2.23 to −1.1 (10−80%) | 1000 | $t_{RES}$ = 3.5 s<br>$t_{REC}$ N/A | speaking, joint bending, walking monitoring | [11] |

| | | | | | | | | |
|---|---|---|---|---|---|---|---|---|
| **Polymeric Micro-structured Substrates** | | | | | | | | |
| PSS:PEDOT-coated PDMS micropyramid array | Drop casting (ex-situ) | 0 − 8 kPa | 23 Pa | $S_1$=10.32 $kPa^{-1}$ (0−3.5 kPa)<br>$S_2$=2.02 $kPa^{-1}$ (3.5−8 kPa) | 800 | $t_{RES}$ = 200 ms<br>$t_{REC}$ = 200 ms | Radial artery pulse measurement | [12] |
| CNT/PDMS microdome array | Premixing (ex-situ) | 0 − 8 kPa | 0.2 Pa | $S_1$=-15.1 $kPa^{-1}$ (0−0.5 kPa) | N/A | $t_{RES}$ = 400 ms<br>$t_{REC}$ = 400 ms | Gas flow, human breathing, voice monitoring | [13] |
| CNT/graphene-coated microstructured PDMS | Dry-transfer (ex-situ) | 0 − 6 kPa | 0.6 Pa | $S_1$=19.8 $kPa^{-1}$ (0−0.3 kPa)<br>$S_2$=0.27 $kPa^{-1}$ (0.3−6 kPa) | 35000 | $t_{RES}$ < 16.7 ms<br>$t_{REC}$ N/A | Bending, torsion, and acoustic signals detection | [14] |
| **Monolithic Conductive Foams** | | | | | | | | |
| Graphene foam | N/A | 0 − 95 %<br>0 − 2 kPa | N/A | $S_1$=229.8 $kPa^{-1}$ (0−0.1 kPa)<br>$S_2$=26.9 $kPa^{-1}$ (0.4−1 kPa) | 1000 | $t_{RES}$ N/A<br>$t_{REC}$ N/A | N/A | [15] |
| Graphene foam | N/A | 0 − 2 kPa | N/A | $S_1$=15.2 $kPa^{-1}$ (0−0.3 kPa) | N/A | $t_{RES}$ N/A<br>$t_{REC}$ N/A | Finger pressure monitoring | [16] |
| Copper nanowire aerogel | N/A | 0 − 60 %<br>0 − 0.2 kPa | 14 Pa | $S_1$=0.7 $kPa^{-1}$ (0.03−0.2 kPa) | 200 | $t_{RES}$ = 80 ms<br>$t_{REC}$ N/A | N/A | [17] |

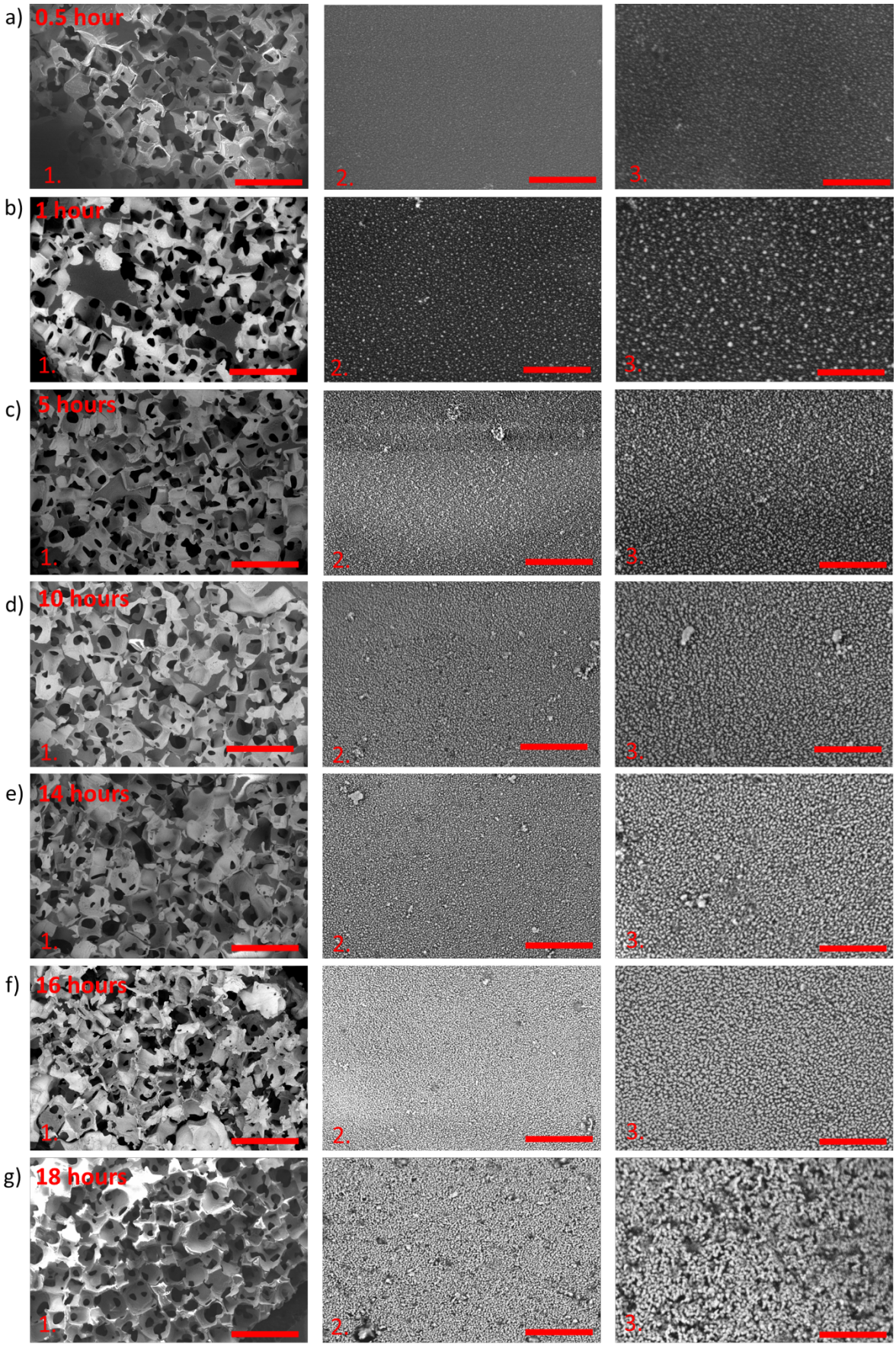


**Figure S1**. Cross-section SEM images of AgNP-coated PDMS foams after 0.5 (a), 1 (b), 5 (c), 10 (d), 14 (e), 16 (f), and 18 (g) hours of decoration at different magnifications: (1) 100×; (2) 50000×, and (3) 100000×. Scale bar is (1) 1 mm, (2) 2 μm, and (3) 1 μm.

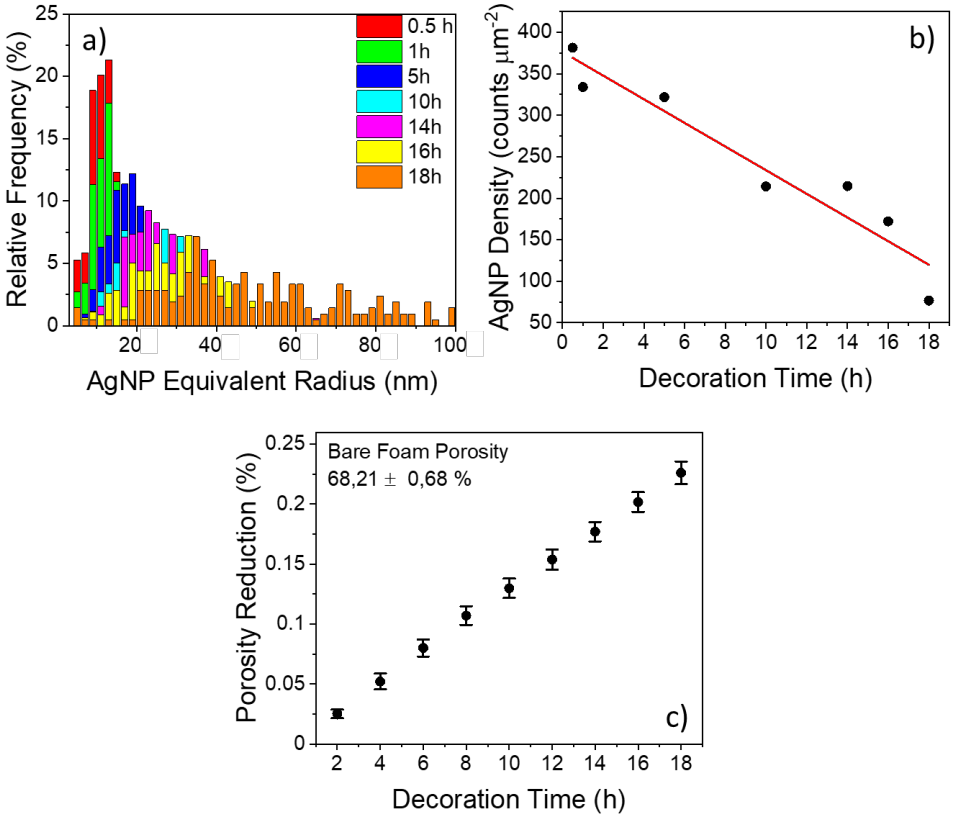


**Figure S2**. AgNP (a) equivalent radius and (b) density of AgNP-coated PDMS foams at different decoration times, evaluated over an area > 12 µm$^2$. (c) Porosity reduction of AgNP-decorated PDMS foams vs. decoration time.

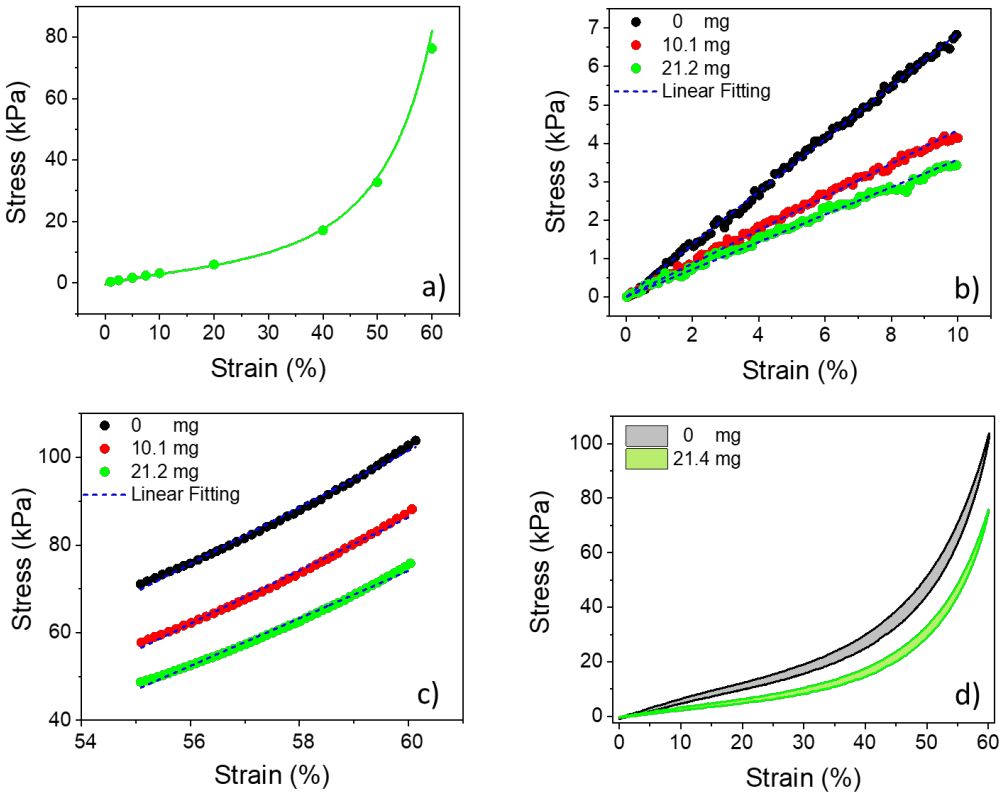


**Figure S3**. (a) Static *vs.* dynamic (strain rate of 0.5 mm $min^{-1}$ ) stress−strain curves of bare PDMS foam. (b) Detail of stress−strain curves at strain values <10 % of bare and AgNP-decorated PDMS foams. Dotted traces represent linear best-fitting of experimental data. (c) Detail of stress−strain curves at strain values >55 % of bare and AgNP-decorated PDMS foams. Dotted traces represent linear best-fitting of experimental data. (d) Hysteresis of the stress-strain curves of bare and AgNP-decorated PDMS foams, highlighting the reduction in the residual energy density of AgNP-coated PDMS foams.

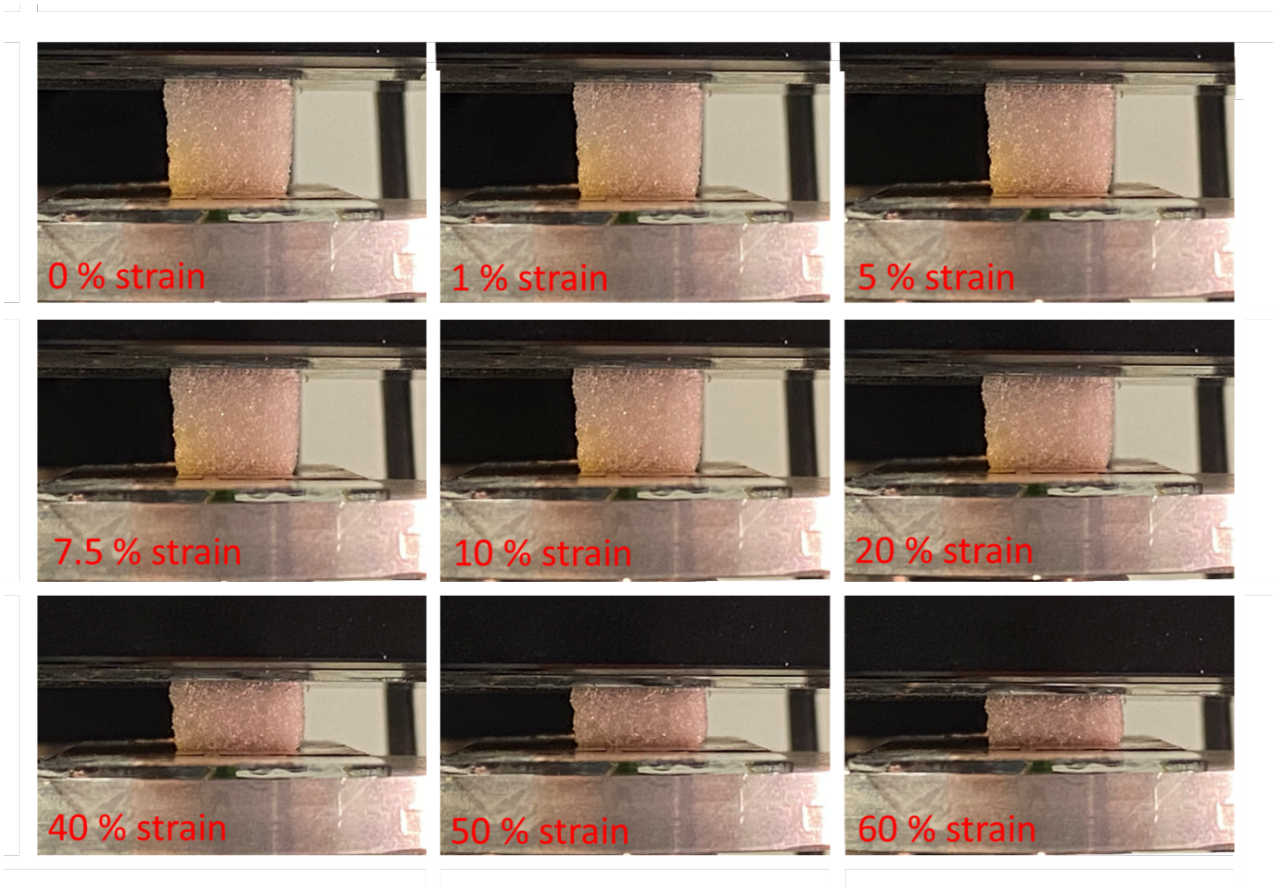


**Figure S4**. Evaluation of the Poisson's ratio of PDMS foams under uniaxial compressive strain in the range 0-60%.

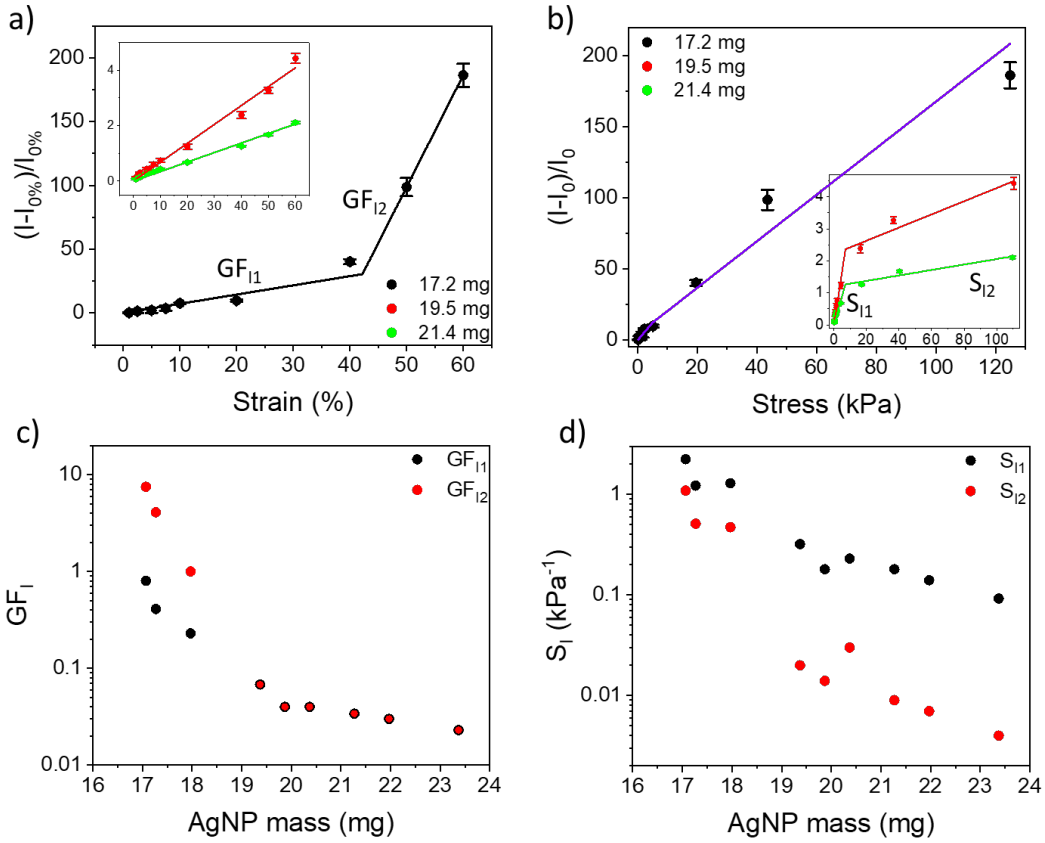


**Figure S5**. (a) Normalized current variation−strain curves of PDMS foams decorated with different AgNP masses; solid lines represent the piecewise linear fitting carried out to retrieve the gauge factor $GF_I$ (i.e., current sensitivity to strain). (b) Normalized current variation−stress curves of PDMS foams decorated with different AgNP masses; solid lines represent the piecewise linear fitting carried out to retrieve the current sensitivity to stress ($S_I$). (c) Gauge factor $GF_I$ (i.e., current sensitivity to strain) *vs.* AgNP mass retrieved from best fitting of experimental data in (a). (d) Current sensitivity to stress ($S_I$) *vs.* AgNP mass retrieved from best fitting of experimental data in (b).

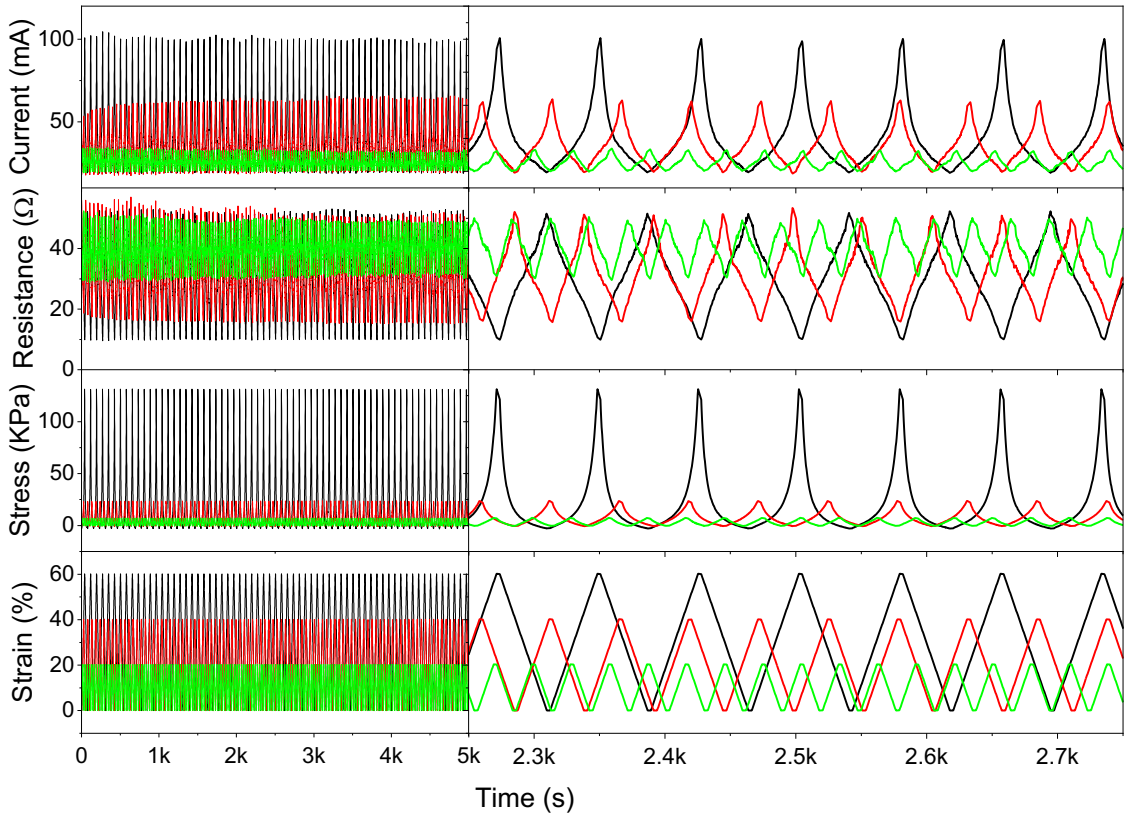


**Figure S6**: Time-resolved experimental data of current, resistance, stress, and strain signals acquired on a PDMS foam decorated with ~19.5 mg of AgNPs at a strain rate of 5 mm $min^{-1}$ over different strain ranges, namely, 0 − 20 % (green lines), 0 − 40 % (red lines), and 0 − 60% (black lines). On the left, the full 5000 s of acquisition; on the right, a detail of 500 s recorded in the middle of the acquisition time.

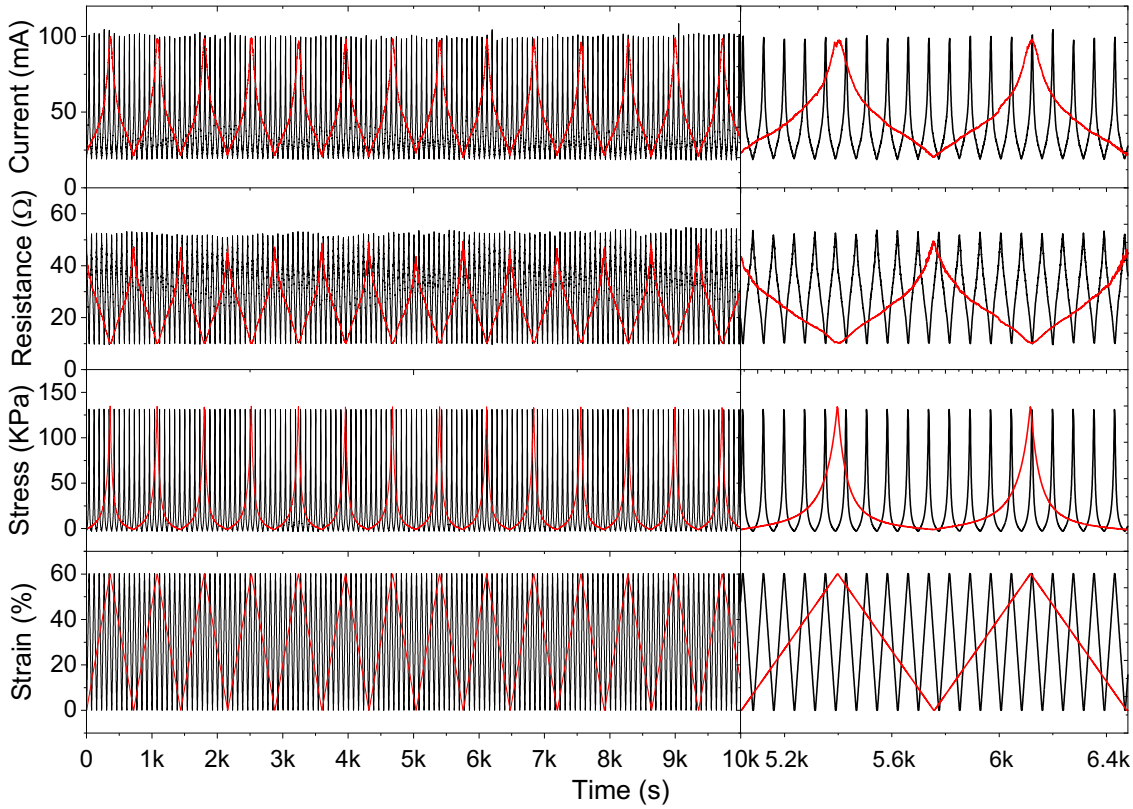


**Figure S7**: Time-resolved experimental data of current, resistance, stress, and strain signals acquired on a PDMS foam decorated with ~19.5 mg of AgNPs at strain rate of 0.5 (red lines) and 5 mm $min^{-1}$ (black lines), over the strain range 0-60%. On the left, the full 10000 s of acquisition; on the right, a detail of 1200 s recorded in the middle of the acquisition time.

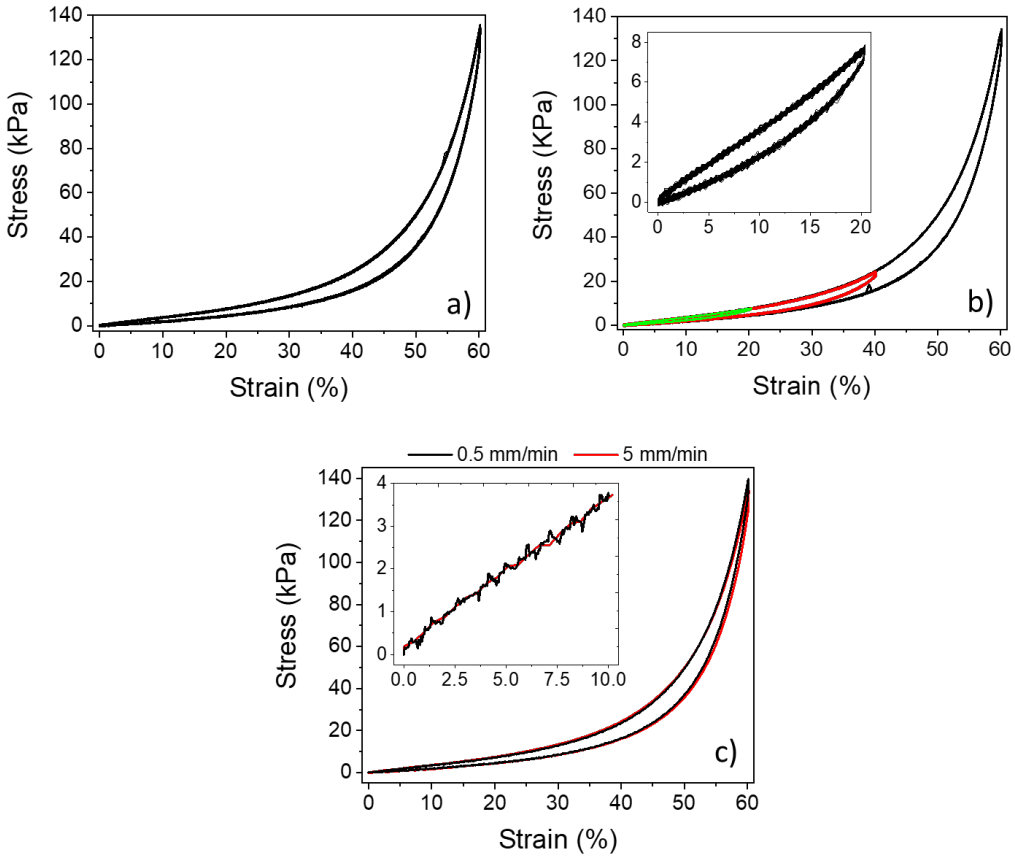


**Figure S8**: (a) Superposition of >1500 stress−strain curves recorded over a time >100 ks on a PDMS foam decorated with ~19.5 mg of AgNPs, measured under uniaxial loading/unloading cycles at a strain rate of 5 mm $min^{-1}$. (b) Superposition of stress−strain curves recorded over a time of 5000 s on a PDMS foam decorated with ~19.5 mg of AgNPs measured under uniaxial loading/unloading cycles at a strain rate of 5 mm $min^{-1}$ over different strain ranges, namely, 0 − 20 % (green lines), 0 − 40 % (red lines), and 0 − 60% (black lines). The inset shows the stress−strain curves measured in the strain range 0 − 20 %. (c) Superposition of stress−strain curves acquired over a time of 10000 s on a PDMS foam decorated with ~19.5 mg of AgNPs measured under uniaxial loading/unloading cycles at a strain rate of 0.5 (black lines) and 5 mm $min^{-1}$ (red lines), over the strain range 0-60%. The inset shows a detail of the stress−strain curves in the strain range 0 − 10 %.

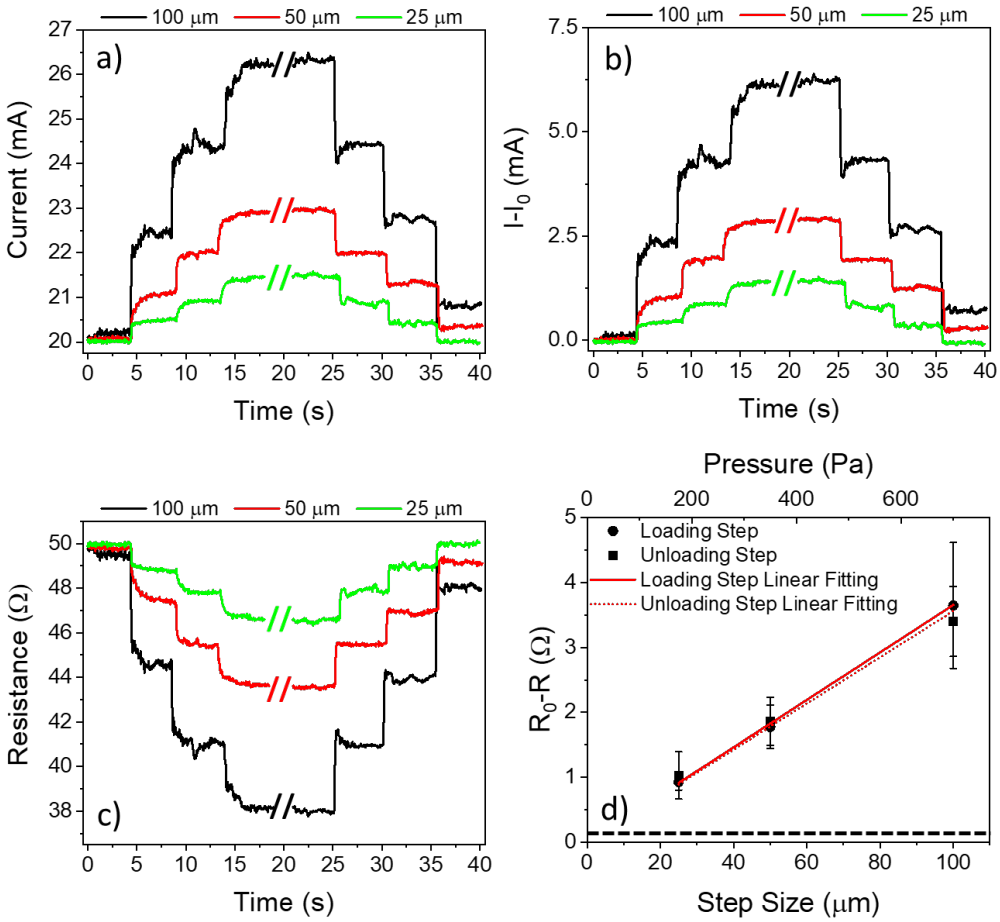


**Figure S9**: Time-resolved current (a), current variation (b), and resistance (c) data measured on a PDMS foam decorated with ~19.5 mg of AgNPs subjected to compression and release steps of 25, 50, and 100 µm (175, 350, and 700 Pa). (d) Resistance variation values (mean ± std) measured on the foams in (a) upon several compression/release steps of 25, 50, and 100 µm (175, 350, 700 Pa). Red solid and dotted lines represent the linear best-fitting of experimental data; the black dotted line represents the noise level at $3.3\sigma_0$.

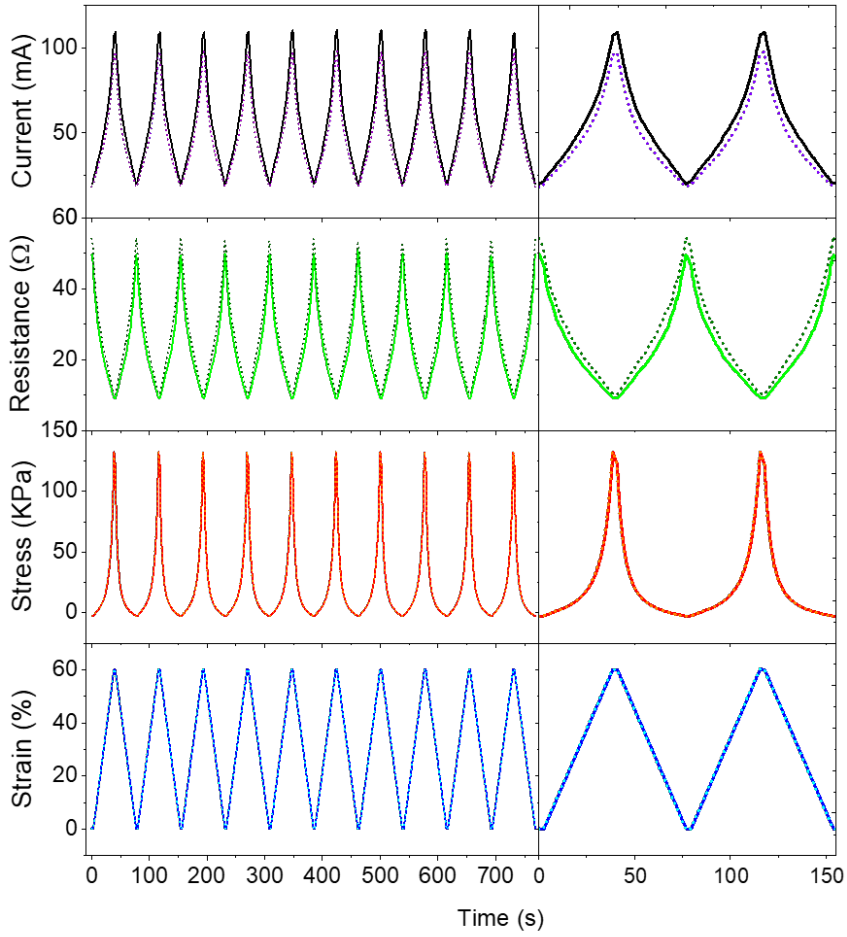


**Figure S10**: Time-resolved experimental raw data (10 full cycles) of current, resistance, stress, and strain acquired at a strain rate of 5 mm $min^{-1}$ over the strain range 0-60% on a PDMS foam decorated with about 19.5 mg of AgNPs right after fabrication and after 6 months from fabrication: (left) full 10 cycles, (right) detail of 2 cycles acquired at the begin of the acquisition. Solid lines refer to data acquired right after fabrication; dotted lines refer to data acquired after 6 months from fabrication.

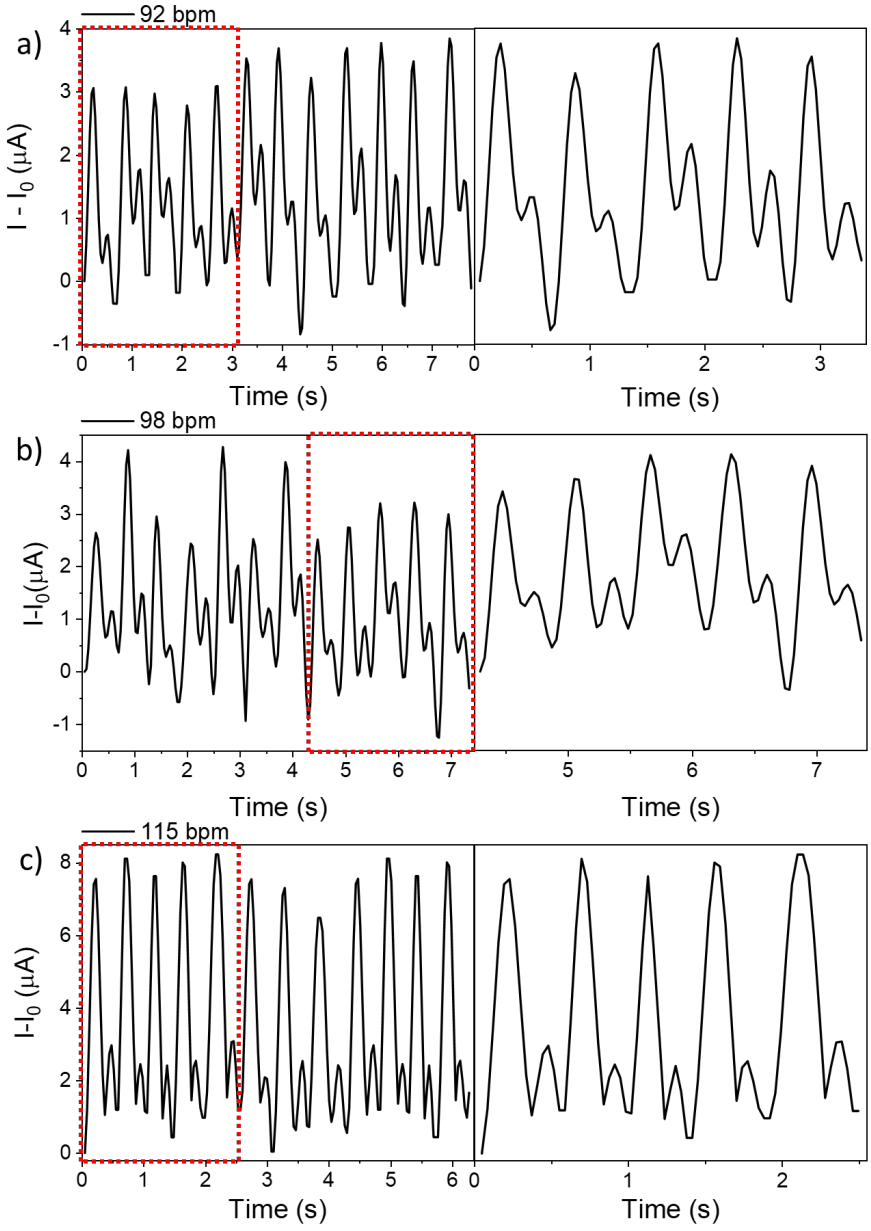


**Figure S11**: Time-resolved current variation acquired on a PDMS foam decorated with ~19.5 mg of AgNPs placed on the right wrist of a 26-year-old male in correspondence of the radial artery. The current signals represent the radial arterial pulse wave measured on the volunteer under rest and stress conditions, namely, 92 bpm (a), 98 bmp (b), and 115 bpm (c).

## References

[1] J. N. Lee, C. Park, and G. M. Whitesides, "Solvent Compatibility of Poly(dimethylsiloxane)-Based Microfluidic Devices," *Anal. Chem.*, vol. 75, no. 23, pp. 6544–6554, 2003.

[2] R. Iglio, S. Mariani, V. Robbiano, L. Strambini, and G. Barillaro, "Flexible Polydimethylsiloxane Foams Decorated with Multiwalled Carbon Nanotubes Enable Unprecedented Detection of Ultralow Strain and Pressure Coupled with a Large Working Range," *ACS Appl. Mater. Interfaces*, vol. 10, no. 16, pp. 13877–13885, 2018.

[3] Y. Wu *et al.*, "Channel Crack-Designed Gold@PU Sponge for Highly Elastic Piezoresistive

Sensor with Excellent Detectability," *ACS Appl. Mater. Interfaces*, vol. 9, no. 23, pp. 20098–20105, Jun. 2017.
[4] H. Bin Yao *et al.*, "A flexible and highly pressure-sensitive graphene-polyurethane sponge based on fractured microstructure design," *Adv. Mater.*, vol. 25, no. 46, pp. 6692–6698, 2013.
[5] S. Chun, A. Hong, Y. Choi, C. Ha, and W. Park, "A tactile sensor using a conductive graphene-sponge composite," *Nanoscale*, vol. 8, no. 17, pp. 9185–9192, 2016.
[6] Y. Luo, Q. Xiao, and B. Li, "Highly compressible graphene/polyurethane sponge with linear and dynamic piezoresistive behavior," *RSC Adv.*, vol. 7, no. 56, pp. 34939–34944, 2017.
[7] Z. Ma *et al.*, "Lightweight, compressible and electrically conductive polyurethane sponges coated with synergistic multiwalled carbon nanotubes and graphene for piezoresistive sensors," *Nanoscale*, vol. 10, no. 15, pp. 7116–7126, 2018.
[8] A. Tewari, S. Gandla, S. Bohm, C. R. McNeill, and D. Gupta, "Highly Exfoliated MWNT-rGO Ink-Wrapped Polyurethane Foam for Piezoresistive Pressure Sensor Applications," *ACS Appl. Mater. Interfaces*, vol. 10, no. 6, pp. 5185–5195, 2018.
[9] X. Wu, Y. Han, X. Zhang, Z. Zhou, and C. Lu, "Large-Area Compliant, Low-Cost, and Versatile Pressure-Sensing Platform Based on Microcrack-Designed Carbon Black@Polyurethane Sponge for Human–Machine Interfacing," *Adv. Funct. Mater.*, vol. 26, no. 34, pp. 6246–6256, 2016.
[10] G. Ge *et al.*, "A flexible pressure sensor based on rGO/polyaniline wrapped sponge with tunable sensitivity for human motion detection," *Nanoscale*, vol. 10, no. 21, pp. 10033–10040, 2018.
[11] Y. Ding, J. Yang, C. R. Tolle, and Z. Zhu, "Flexible and Compressible PEDOT:PSS@Melamine Conductive Sponge Prepared via One-Step Dip Coating as Piezoresistive Pressure Sensor for Human Motion Detection," *ACS Appl. Mater. Interfaces*, vol. 10, no. 18, pp. 16077–16086, 2018.
[12] C. L. Choong *et al.*, "Highly stretchable resistive pressure sensors using a conductive elastomeric composite on a micropyramid array," *Adv. Mater.*, vol. 26, no. 21, pp. 3451–3458, 2014.
[13] J. Park *et al.*, "Giant tunneling piezoresistance of composite elastomers with interlocked microdome arrays for ultrasensitive and multimodal electronic skins," *ACS Nano*, vol. 8, no. 5, pp. 4689–4697, 2014.
[14] M. Jian *et al.*, "Flexible and Highly Sensitive Pressure Sensors Based on Bionic Hierarchical Structures," *Adv. Funct. Mater.*, vol. 27, no. 9, 2017.
[15] L. Lv, P. Zhang, T. Xu, and L. Qu, "Ultrasensitive Pressure Sensor Based on an Ultralight Sparkling Graphene Block," *ACS Appl. Mater. Interfaces*, vol. 9, no. 27, pp. 22885–22892, 2017.
[16] C. Hou, H. Wang, Q. Zhang, Y. Li, and M. Zhu, "Highly conductive, flexible, and compressible all-graphene passive electronic skin for sensing human touch," *Adv. Mater.*, vol. 26, no. 29, pp. 5018–5024, 2014.
[17] X. Xu *et al.*, "Copper Nanowire-Based Aerogel with Tunable Pore Structure and Its Application as Flexible Pressure Sensor," *ACS Appl. Mater. Interfaces*, vol. 9, no. 16, pp. 14273–14280, 2017.